Chapter 5

Optimization of process parameters for torrefaction of A*cacia nilotica* using response surface methodology and characteristics of torrefied biomass as upgraded fuel

General background

This chapter dealt with the optimization of process parameters for torrefaction *Acacia nilotica* (TAN) using response surface methodology. The temperature (220-280 ℃), retention time (20-60 min), and heating rate (5-15 ℃/min) were selected as independent variables and energy yield and higher heating value of TAN were selected as dependent variables. The ANOVA and regression analysis were used to study the fitness of developed model using central composite design technique. In addition, the characteristics of torrefied biomass at optimized condition were tested using TGA, FTIR, XRD, BET, and SEM analysis and compared with DAN. Moreover, the fuel characteristics like fuel ratio (FR), combustibility index (CI), volatile ignitability (VI), flow behavior through angle of repose, Hausner ratio (HR), Carr compressibility index (CCI), cohesion coefficient (C), moisture sorption ability and densities (bulk, tapped and particle) of TAN at optimized condition and DAN were also compared.

5.1 Introduction

Torrefaction is used as a pretreatment step which produces high-quality solid biofuel as torrefied biomass. This torrefied biomass can be used in different thermochemical conversion processes like pyrolysis, gasification and combustion to increase the quality of products such as high-grade bio-oil (Dai et al., 2019) and producer gas (Bach et al., 2019) with the lower harmful emission (Louwes et al., 2017) during the process. Therefore, the overall efficiency of the thermochemical process can be increased by using torrefied biomass (Dai et al., 2019). The process of torrefaction depends not only on biomass structure (amount of cellulose, hemicellulose and lignin) and ash content (Lee et al., 2012) but also depends on the process parameters like temperature, heating rate, retention time (Buratti et al., 2018), particle size (Dai et al., 2019). Chen et al. (Chen & Kuo, 2011) suggested that torrefaction process is highly influenced by temperature rather than retention time. Generally, as the temperature increases during torrefaction, more volatiles are released due to the conversion of oxygen-containing compound. The variation of solid yield and higher heating value (HHV) of torrefied biomass with retention time is marginal at fixed temperature (Buratti et al., 2018). Also, EY and HHV of solid product are important outcomes of the process. However, energy yield (EY) and HHV reflect opposite trend, when process parameters are varied during the process. Thus, optimizing the process parameters and a balance between EY and HHV becomes quite important for energy densification and energy utilization. Optimization may reduce operational cost regarding scale-up of the process at industrial level. Thus considering torrefied *Acacia nilotica* (TAN) as desired product from torrefaction, optimization of process parameters such as temperature, retention time and heating rate for HHV and EY of TAN was performed using

RSM. The ANOVA and regression analysis were used to study the fitness of developed model using central composite design technique. Response surface methodology (RSM) is one of the most prevalent and promising techniques to develop, improve, and optimize the process parameters and their interaction effect on the process with a minimum number of experiments. It was developed by Box and Wilson in 1951 (Dhanavath et al., 2017). It is a statistical and mathematical (Gholami et al., 2019) technique having a multivariable non-linear model, which generally is used to optimize the process parameters. In it, a mathematical model is developed which, best fits the experimental data (Cotana et al., 2015). The optimum values of responses are obtained using developed model.

5.2 Material and methods

5.2.1 Sample preparation

The detailed discussion about the collection of *Acacia nilotica* and preparation of dried *Acacia nilotica* (DAN) has been discussed in Chapter 3.

5.2.2 Experimental design using RSM

For optimization of parameters, RSM was used. A three-factor face central composite design, a kind of RSM technique was used to optimize the response in the process. The central composite design technique is well suited for fitting a quadratic surface, which usually works well for any process optimization. This technique is being widely used since it provides a minimum number of experimental run for optimizing the response variable and an easy way to estimate the interaction between different parameters. Assuming the experiments will be performed in a single day with one block, twenty experiments have to be performed, which may be derived from Eqs. (5.1) (Tan et al., 2008), comprising eight factorial points (2^n), six axial points (2n) and six replicates at center points (n_c).

$$N = 2^n + 2n + n_c = 2^3 + 2(3) + 6 = 20 \qquad (5.1)$$

where N is the total number of experiments that have to be performed, n is the number of independent variables and n_c is the number of replicates at central points.

The central point varies between 3 to 10 and it can be used to predict experimental error and reproducibility of data. Temperature (A), retention time (B) and heating rate (C) of range 220-280 ℃, 20-60 min and 5-15 ℃/min, respectively were selected as independent variables. Code -1, 0 and +1 were the value of temperature (220, 250 and 280 ℃), retention time (20 min, 40 min and 60 min) and heating rate (5, 10, and 15 ℃/min). HHV and EY of TAN were chosen as response and both the responses have to be maximized. The matrix of experimental design is given in Table 5.1. The experimentally calculated HHV and EY are incorporated in design expert software (Stat-Ease Design-Expert version-11) as the actual value. While predicted and residual values obtained by software. Data obtained from the experiments were used to optimize the selected parameter. The suggested mathematical model having highest polynomial degree was chosen from central composite design and also it should not be aliased (B. Gratuito et al., 2008).

Once the experiments have been performed, the response variables (HHV and EY of TAN) were correlated with independent parameters (temperature, retention time and heating rate). The general relationship between response and independent variable is given as:

$$Y = f(X_1, X_2, X_3, \ldots\ldots\ldots, X_n) \qquad (5.2)$$

where Y is the response variable, f is the function relating response to independent variable and X_1, X_2, X_3,…….. X_n are the n independent variables which affect the response.

Following the second order polynomial equation as suggested by central composite design technique, the generalized form of second order polynomial equation is given as:

$$Y = b_0 + \sum_{i=1}^{k} b_i X_i + \sum_{i=1}^{k} b_{ij}\ X_i^2 + \sum_{i_{i>j}}^{k} \sum_{j}^{k} b_{ij} X_i\, X_j \quad (5.3)$$

where i is the linear coefficient, j is the quadratic coefficients, b is the regression coefficient, k is the number of factors that were studied and optimized in the study.

The ANOVA and regression analysis were used to study the fitness of regression model at 95% confidence level using Design-Expert software. This analysis was used to check the deviation of mean. Set of experimental data were analyzed in accordance with several variables like p value, degree of freedom (DF), F value, determination coefficient (R^2), predicted determination of coefficient (R^2_{pred}) and adjusted determination of coefficient (R^2_{adj}) to check the statistical fitness of the model. From ANOVA, F and p values are used to examine the importance of terms appeared in the model equation. F value suggests that variation in responses can be demonstrated by regression equation, whereas, p value specifies, whether F value is large enough to ascertain statistical importance of the developed model. For that matter, p value for model should be less than 0.05 and p value for lack of fit test should be greater than 0.05 (Dhanavath et al., 2017). Three dimensional RSM plots and contour plots were incorporated to analyze the effect of each variable and their interaction with HHV and EY of TAN.

5.2.3 Experimental setup and torrefaction procedure

The detail about the experimental set-up and torrefaction process has been discussed in Chapter 3. The torrefaction of DAN was carried out following the experimental matrix given in Table 5.1. The TAN is considered as the main product in this study. The TAN yield was calculated using Eqs. (5.4).

$$\text{TAN yield (wt\%)} = \frac{\text{Weight of TAN (g)}}{\text{Weight of DAN (g)}} \times 100 \qquad (5.4)$$

Energy yield is a function of solid product yield and their HHV. EY can be calculated using Eqs. (5.5).

$$\text{Energy yield} = (\text{TAN yield}) \times \frac{\text{HHV}_{\text{db,TAN}}}{\text{HHV}_{\text{db,DAN}}} \qquad (5.5)$$

Table 5.1 Experimental design matrix and actual, predicted and residual value of responses obtained using RSM

	Level of actual variable			**Actual, predicted and residual value of response**					
Run	T (^{o}C)	RT (min)	HR (^{o}C/min)	**HHV (MJ/kg)**			**EY (%)**		
				Actual value	Predicted value	Residual value	Actual value	Predicted Value	Residual value
1	250	40	10	22.46	22.51	-0.0453	70.02	69.75	0.2677
2	250	40	10	22.38	22.44	-0.0557	70.52	69.85	0.5722
3	250	40	10	21.77	21.98	-0.2151	69.78	69.39	0.3857
4	220	60	15	20.71	20.71	0.0030	75.55	76.01	-0.4545
5	220	20	15	19.61	19.49	0.1190	75.95	74.83	1.1200
6	250	40	5	23.02	22.68	0.3369	71.31	70.17	1.1300
7	220	20	5	19.97	20.02	-0.0530	76.35	76.98	-0.6337

8	280	20	15	24.39	24.33	0.0600	49.72	49.28	0.4374
9	250	60	10	23.58	23.36	0.2249	71.96	71.18	0.7754
10	280	40	10	25.36	25.25	0.1109	49.76	50.77	-1.0100
11	220	40	10	20.32	20.30	0.0249	75.57	75.36	0.2054
12	250	40	10	22.54	22.72	-0.1766	70.32	69.65	0.5799
13	250	40	10	21.99	22.11	-0.1347	69.88	69.67	0.2165
14	280	60	5	26.19	26.34	-0.1530	51.72	52.64	-0.9187
15	280	20	5	24.73	24.77	-0.0370	53.21	52.55	0.6553
16	220	60	5	21.18	21.27	-0.0940	76.04	76.28	-0.2366
17	250	40	10	22.77	22.94	-0.1724	71.23	70.98	0.2544
18	250	20	10	21.87	21.96	-0.0891	68.97	70.55	-1.5800
19	280	60	15	25.89	25.87	0.0190	52.08	51.25	0.8345
20	250	40	15	21.98	22.18	-0.2011	66.47	68.40	-1.9400

5.2.4 Characteristics of raw and torrefied biomass

The detailed discussion about proximate and ultimate analysis, fuel and flow properties, density, thermogravimetric analysis, Scanning electron microscopy, FTIR analysis has been discussed in Chapter 3. Additionally, the Brunauer–Emmett–Teller (BET) surface area of TAN252-60-5 was determined on an ASAP 2020 adsorption apparatus (Micromeritics, USA). Nitrogen gas was used as an adsorbate. Prior to analysis, the torrefied biomass sample was degassed at −180 ℃ for 24 h. The crystallinity of the DAN and TAN at optimized condition was investigated using X-ray diffractometer (mini flux II, Rigaku, Japan) with a scanning rate of 5^{o} per min with a step size of 0.02^{o} in the range of 0 to 80^o (2θ). The crystallinity index and crystal size were calculated using following Eqs. (5.6)

$$\text{CrI}(\%) = \left(\frac{I_{002} - I_{am}}{I_{002}}\right) \times 100 \quad (5.6)$$

where CrI denotes crystallinity index; I_{002} and I_{am} denote crystalline and amorphous intensity, respectively of diffraction plane (002).

$$L_{002} = \frac{k \times \lambda}{\beta \times \cos\theta} \quad (5.7)$$

where L_{002} denotes the crystal size, k denotes the Scherrer constant (0.90), λ denotes the X-ray wavelength, usually which is 0.15406 nm, β denotes the full width at half maximum (FWHM) of peak, and θ denotes the diffraction angle plane (002) (Zheng et al., 2015).

5.3 Results and discussion

5.3.1 Solid product yield and Energy yield

The fraction of each product depends on operating parameter like temperature, retention time, heating rate. Maximum and minimum solid yield (73.82% and 38.13%) were obtained at temperature (220 and 280 ℃), retention time (20 and 60 min), and heating rate (5 ℃/min), respectively. The cause of decrease in solid yield with temperature has been discussed in Chapter 3. EY gives an indication about the amount of energy preserved in biomass after torrefaction. The EY of TAN decreases with temperature at constant retention time and heating rate. Maximum and minimum EY (76.35% and 49.72%) were obtained at temperature (220 and 280 ℃), retention time (20 min), and heating rate (5 and 15 ℃/min), respectively. As the retention time increases, the yield of liquid and non-condensable gases increased. At a fixed temperature and longer retention time, biomass is exposed for longer duration, hence, yield of liquid and gas enhanced. Higher retention time also favors the devolatilization reaction, which can increase the yields of liquid product and gases.

5.3.2 Response surface analysis for HHV and EY of Torrefied biomass

The relation between experimental and predicted values of HHV and EY of TAN are shown in Fig. 5.1 (a) and (b), respectively. It shows that both values are close to each other, indicating that the developed model is well suited to establish the relation between dependent and independent variables during torrefaction process. This relationship can also be justified by the value of correlation coefficient (R^2), which varies between zero to one. The value of coefficient close to one indicates lesser error in developed model.

(a) **(b)**

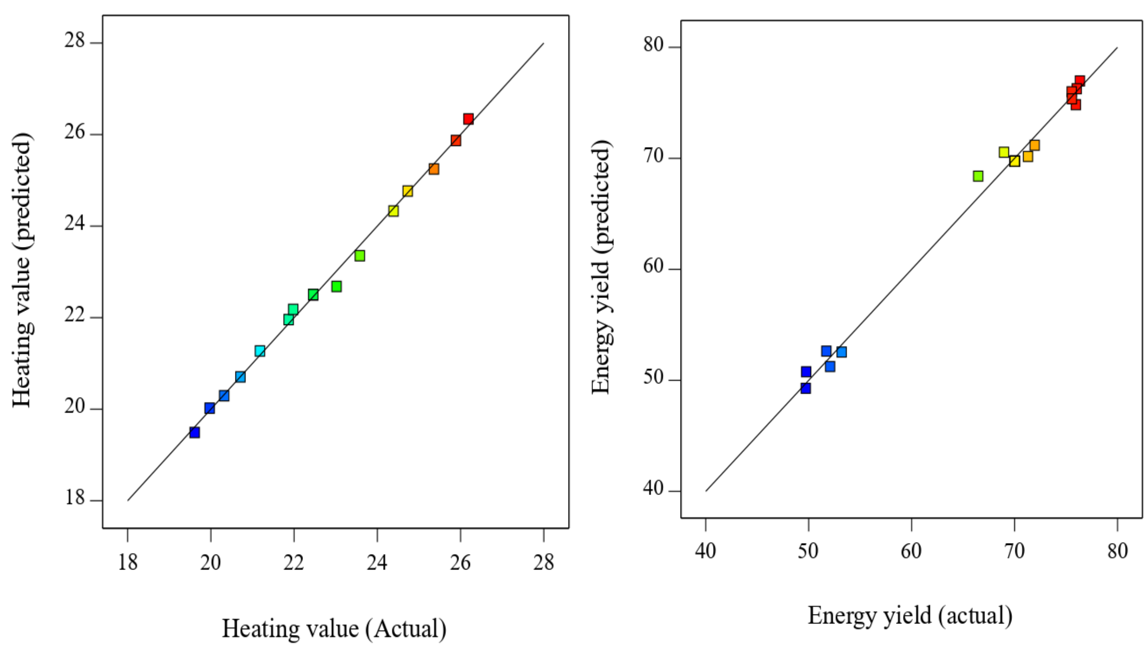

Figure 5.1 Relationship between actual and predicted values of model (a) HHV and (b) EY

For present model, values of correlation coefficients for HHV and EY of TAN are 0.9957 and 0.9921, respectively, indicating a good correlation between independent and dependent variables. The relation between dependent parameter (HHV) and independent parameters (temperature (A), retention time (B), and heating rate (C)) obtained in this study is:

$$Y_{HHV}\ (\text{MJ/kg}) = +21.2581 - 0.7266A - 0.0284B - 0.0277C + 0.0001AB + 0.0001AC - 0.00008BC + 0.00002A^2 + 0.0003B^2 - 0.0002C^2 \quad (5.8)$$

The statistical analysis of HHV is given in Table 5.2. The significance of each independent variable on the response can be analyzed using F-value and p-value. For a significant model, the p-value should be less than 0.05 and F- value should be large. For present model, p-value and F-values are <0.0001 and 256.54 for HHV, suggesting that the developed model is applicable. The p-value and F-value of model can also be used to compare the linear term (A, B, C), interaction term (AB, AC, BC), and quadratic term (A^2, B^2, C^2). For HHV of TAN linear term (A, B and C) and quadratic term (A^2) are significant having p-value <0.0001, <0.0001 0.0009, and 0.0270 respectively. The F-value of all the significant terms (A, B, C, and A^2) is 2099.53, 166.72, 21.56 and 6.70, respectively. It can be concluded that for HHV of TAN, temperature has a larger effect on the process than retention time and heating rate.

Table 5.2 ANOVA for quadratic model of response: **HHV and EY**

Source	Sum of square	Degree of freedom	Mean of square	F-value	p-value	Remark
HHV						
Model	67.47	9	7.50	256.54	< 0.0001	Significant
A-Temperature	61.36	1	61.36	2099.53	< 0.0001	
B- Retention time	4.87	1	4.87	166.72	< 0.0001	
C-Heating rate	0.6300	1	0.6300	21.56	0.0009	
AB	0.0528	1	0.0528	1.81	0.2085	
AC	0.0045	1	0.0045	0.1544	0.7026	
BC	0.0006	1	0.0006	0.0210	0.8878	
A^2	0.1958	1	0.1958	6.70	0.0270	
B^2	0.0634	1	0.0634	2.17	0.1716	
C^2	0.0147	1	0.0147	0.5040	0.4940	
Residual	0.2922	10	0.0292			
Lack of Fit	0.2922	5	0.0584	4.58	0.0569	
Pure Error	0.0000	5	0.0000			
Cor Total	67.76	19				
R^2 0.9957		Adjusted R^2 0.9918		Predicted R^2 0.9681		
EY						
Model	1724.53	9	191.61	139.88	< 0.0001	Significant
A-Temperature	1512.10	1	1512.10	1103.88	< 0.0001	
B- Retention time	0.9912	1	0.9912	0.7236	0.4149	
C-Heating rate	7.82	1	7.82	5.71	0.0380	
AB	0.3121	1	0.3121	0.2279	0.6434	

AC	0.6280	1	0.6280	0.4584	0.5137	
BC	1.76	1	1.76	1.29	0.2831	
A^2	122.70	1	122.70	89.57	< 0.0001	
B^2	3.44	1	3.44	2.51	0.1440	
C^2	0.5822	1	0.5822	0.4250	0.5292	
Residual	13.70	10	1.37			
Lack of Fit	13.70	5	2.74	6.68	0.0647	
Pure Error	0.0000	5	0.0000			
Cor Total	1738.23	19				
R^2 0.9921		Adjusted R^2 0.9850		Predicted R^2 0.9244		

Three dimensional (3D) and contour plots of response at optimized condition were obtained in this study to verify the dependence of HHV of TAN with different process parameters like temperature, retention time and heating rate (Fig. 5.2). In case of three independent variables, it is not possible to show the effect of all variable on the response simultaneously. Hence the effect of two variables keeping third as constant is shown in this study. Figs. 5.2 (a) and (b) show the 3D and contour plots for variation of HHV of TAN with respect to temperature and retention time. It can be seen that at a constant heating rate of 5 ℃/min, the HHV of TAN increases up to a maximum value, with increase in temperature and retention time. Similar results can be obtained in case of variation of HHV of TAN with temperature and heating rate at a constant retention time of 60 min (Figs. 5.2 (c) and (d)). It can be concluded that maxima of HHV of TAN can be obtained in case of higher temperature, retention time and heating rate. A flat 3D surface can be seen in Figs. 5.2 (e) and (f) confirming that HHV of TAN does not vary too much with an increase in retention time and heating rate at particular temperature (250 ℃). In can be mentioned that torrefaction is more temperature driven process than retention time and heating rate. Thus, properties like HHV and EY are highly dependent on temperature than the retention time and heating rate. With an increase in temperature, relative increase in carbon content and a decrease in oxygen content lead to increase in HHV of biomass.

(a)

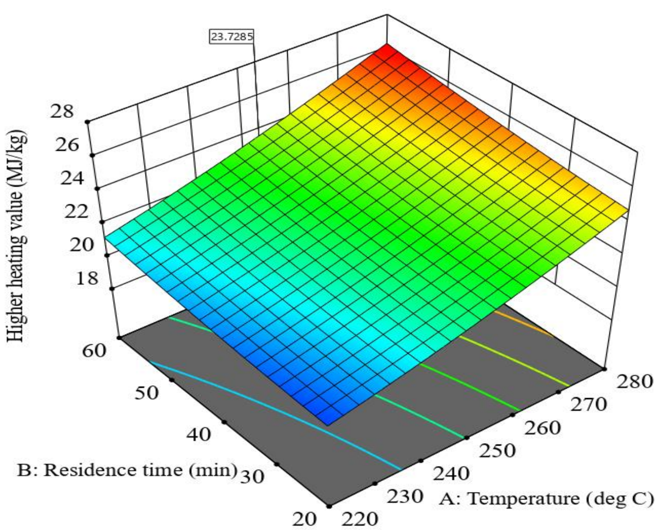

(b)

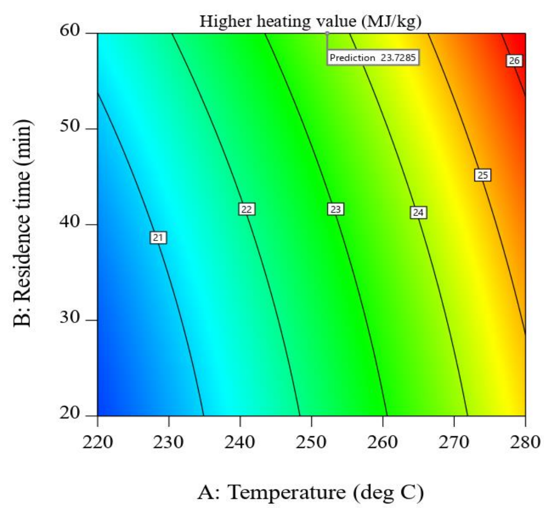

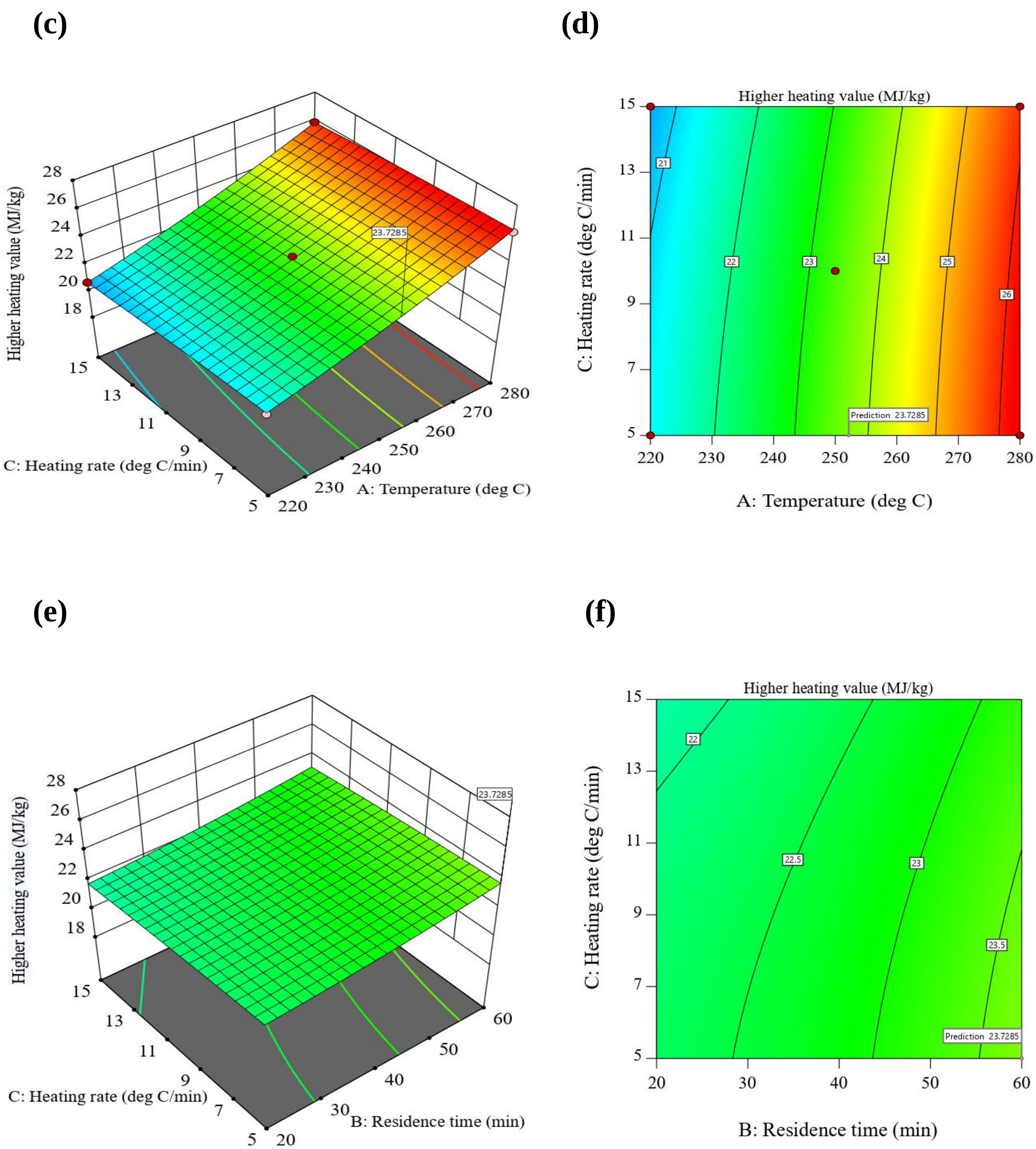

Figure 5.2 Three dimensional response surface and contour plots of HHV showing the effect of (a) and (b) temperature and retention time; (c) and (d) temperature and heating rate; (e) and (f) heating rate and retention time.

For EY, relation between dependent and independent (temperature, retention time and heating rate) variable is as follows:

$$Y_{EY} (\%) = +3.3065A - 0.3372B + 0.4703C + 0.0003AB - 0.0018AC + 0.0046BC$$

$$-0.0074A^2 + 0.0027B^2 - 0.0184C^2 - 287.3708 \qquad (5.9)$$

The statistical analysis for EY is given in Table 5.2. For developed model in case of EY, p-value and F-value are <0.0001 and 139.88, suggesting that developed model is significant. For EY of TAN, linear term (A and C), and quadratic term (A^2) are significant, having p-values <0.0001, 0.0380, and <0.0001, respectively. In case of EY, the F values for significant terms (A, C, and A^2) are 1103.88, 5.71, and 89.57, respectively. The dependency related to temperature is similar to HHV; however EY has the different trend relative to retention time and heating rate. In case of EY, the process is more dependent on heating rate than retention time.

Fig. 5.3 shows the 3D and contour plots for response EY at optimized condition with respect to independent variables. Figs. 5.3 (a), (b) and (c), (d) show the coupled effect of temperature- retention time at constant heating rate of 5 °C/min and temperature-heating rate at constant retention time of 60 min, respectively on EY. It was found that the maximum value of EY can be obtained at lower temperature, retention time and heating rate during torrefaction process. A flat 3D surface can be seen confirming that EY of TAN does not vary too much with an increase in retention time and heating rate at a particular temperature (Figs. 5.3 (e) and (f)). At lower temperature, the degradation of hemicellulose is less and almost insignificant for cellulose and lignin (Dai et al., 2019) due to lower rate of devolatilization. Hence, mass loss is very small.

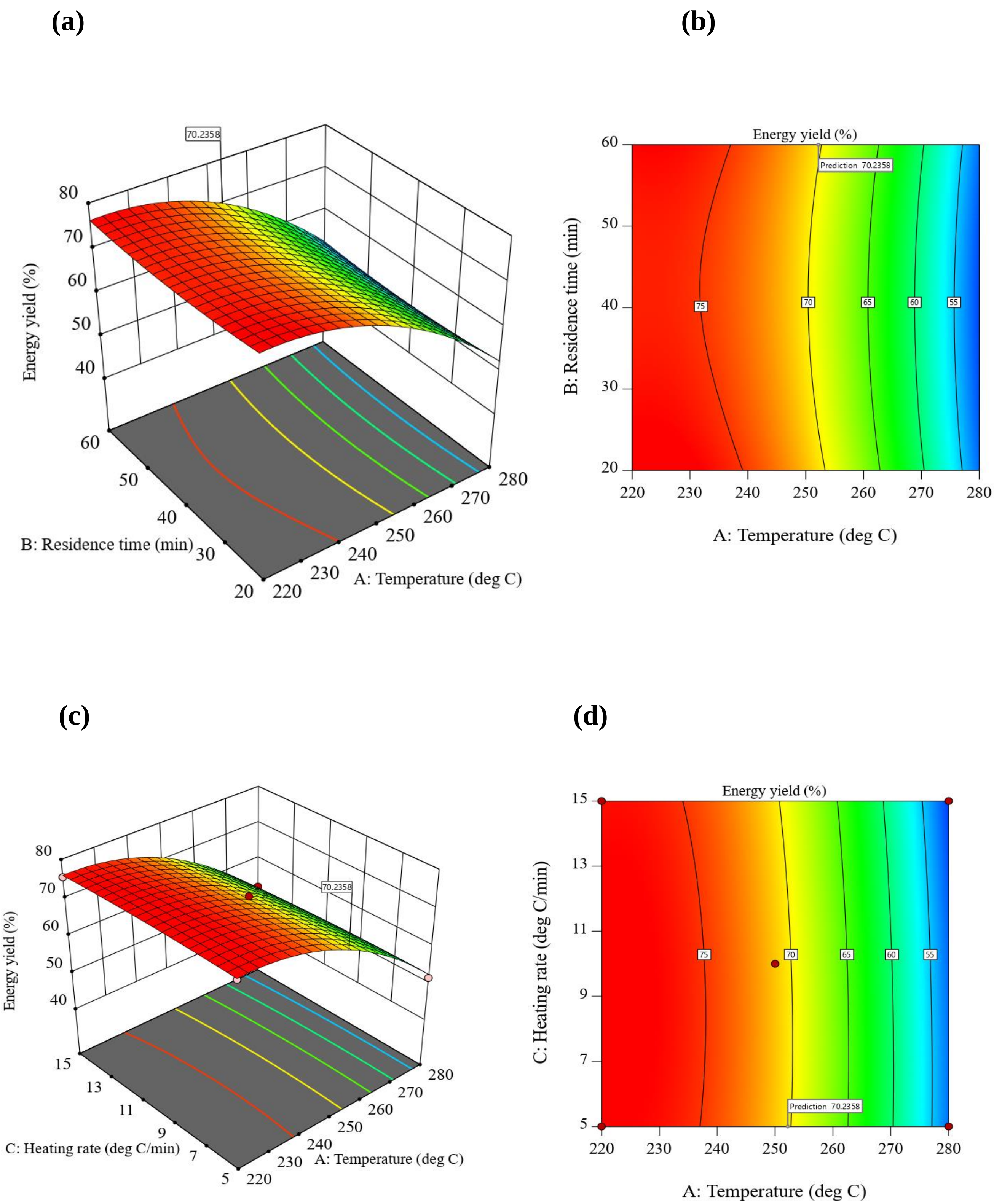
(a)
(b)
70.2358
Energy yield (%)
80
70
60
50
40
B: Residence time (min)
60
50
40
30
20
A: Temperature (deg C)
220
230
240
250
260
270
280
Energy yield (%)
Prediction 70.2358
75
70
65
60
55
(c)
(d)
C: Heating rate (deg C/min)
15
13
11
9
7
5

(e) **(f)**

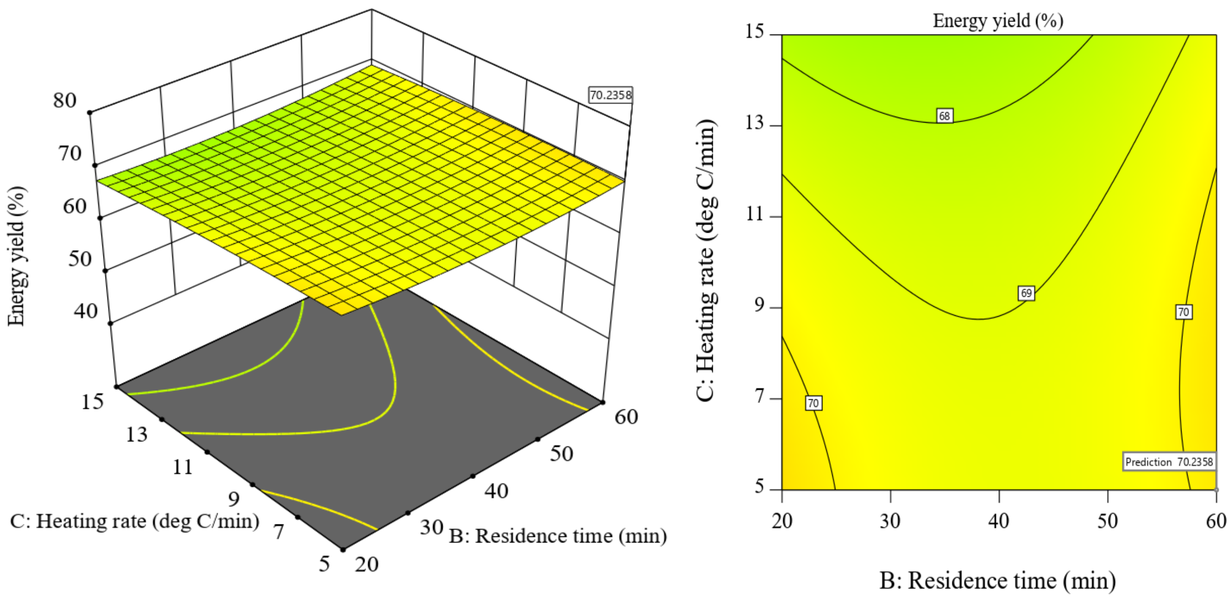

Figure 5.3 Three dimensional response surface and contour plots of EY showing the effect of (a) and (b) temperature and retention time; (c) and (d) temperature and heating rate; (e) and (f) heating rate and retention time.

5.3.3 Optimization of HHV and EY of Torrefied biomass

Twenty experiments have been performed according to the experimental matrix given in Table 5.1. The maximum HHV (25.87 MJ/kg) of TAN was found at 280 °C, 57 min retention time and 5 °C/min heating rate (Table 5.3). On the other hand, maximum EY (75.14 %) was obtained at 220 °C, 20 min retention time and 10 °C/min heating rate (Table 5.3). It is evident that both HHV and EY attain maximum value at different set of conditions. It may be mentioned that EY indicates energy densification, whereas HHV refers to the direct utilization potential of TAN as solid fuel. Maximum HHV at minimum

EY would be beneficial for using TAN as solid fuel. While maximum EY at minimum HHV would be required in case of biomass densification. In the present study, there was a need to maximize both HHV and EY. As predicted by RSM, the maximum value of HHV and EY are 23.73 MJ/kg and 70.20 %, respectively, obtained at 252 °C, 60 min retention time and 5 °C/min heating rate. For validating these data, experiments were performed and it can be seen that the error is less than 2 % (Table 5.3). This clearly suggests that the developed model is in good agreement with the experimental findings.

Table 5.3 Experimental and predicted values of responses at optimum condition

Parameter	Required optimum values		
	Maximum HHV and Minimum EY	**Minimum HHV and Maximum EY**	**Maximum HHV and Maximum EY**
Temperature (°C)	280	220	252
Retention time (min)	57	20	60
Heating rate (°C/min)	5	10	5
HHV (MJ/kg) (measured)	25.86	19.98	24.06
HHV (MJ/kg) (predicted)	26.19	19.82	23.73
Error (%)	−1.2	0.8	1.3
Energy yield (%) (measured)	52.91	75.14	71.31
Energy yield (%) (predicted)	52.33	76.34	70.20
Error (%)	1.1	−1.3	1.5
Desirability (%)	98.30	99.40	69.04

5.3.4 Physical and chemical properties of raw and torrefied biomass

The proximate and ultimate analyses data along with HHV and EY at optimized condition are presented in Table 5.4, which clearly shows that MC and VM both decreased as the temperature increased during torrefaction. MC for DAN is 6.24 %, while 1.67 % TAN252-60-5. Besides, the VM also decreased from 80.36% for DAN to 44.78% for TAN252-60-5. The AC of biomass increased from 0.65% for DAN to 1.42% for TAN252-60-5. Ash has strong affinity to deposit in the boiler, pyrolyzer, and gasifier (Cai et al., 2017). So it will be helpful to know the physical and chemical characteristic of ash to prevent such problems of deposition. The FC increased from 12.75% for DAN to 52.13% for TAN252-60-5. This increase in FC and AC was observed during torrefaction because as the temperature increases, rate of devolatilization of (water vapour, methane, ethane, and other lighter hydrocarbon) from biomass also increases which results in relative decrease in MC and VM and relative increase in FC and AC. During torrefaction, loss of hydrogen and oxygen are more compared to the loss of carbon. The relative increase in the carbon content of biomass during torrefaction is responsible for higher HHV. The HHV obtained for DAN, and TAN252-60-5 are 19.31, and 24.06 MJ/kg, respectively. These results are in good agreement with the published literature for similar feedstock.

Table 5.4 Characteristics of DAN and TAN252-60-5

Analysis	DAN	TAN252-60-5
MC (wt%)	6.24	1.67
AC (wt%)	0.65 (0.69)	1.42 (1.44)
VM (wt%)	80.36 (85.70)	44.78 (44.54)
FC (wt%)	12.75 (13.59)	52.13 (53.01)
O/C	1.09	0.60
H/C	0.17	0.08
HHV (MJ/kg)	19.31 (20.59)	23.73 (24.13)
Solid yield (%)	-	59.90
EY (%)	-	70.22
Geometric mean diameter (mm)	0.53	0.43
FR	0.15	1.19
CI (MJ/kg)	149.43	21.93
VI (MJ/kg)	17.39	13.44
Angle of repose (degree)	38.89	35.75
HR	1.29	1.21
CCI	22.48	17.35
C	0.40	0.35
Bulk density (kg/m^3)	231.45	193.48
Tapped density (kg/m^3)	300.71	235.67
Particle density (kg/m^3)	1251	1156
BET surface area (m^2/g)	-	0.9703
Pore volume (cm^3/g)	-	0.0015
Mean pore diameter (nm)	-	13.69

5.3.5 Fuel and flow properties of torrefied biomass

Table 5.4 presents the combustion indices of the biomass, which are commonly used as crucial parameters in thermochemical conversion processes. In coal-firing power plants, the recommended value of FR is between 0.5-3.0. The FR for DAN and TAN252-60-5 are 0.15 and 1.19, respectively. With increase in temperature, FR of DAN increases since fixed carbon content increases along with decrease in volatile matter. The fuel having higher FR leads to increase in unburnt portion of the fuel, which decreases boiler efficiency during the operation. The fuel which has FR greater than 2 can cause ignition and flammability problem during the application. The reported range of CI and VI for coal are: CI should be less than 23MJ/kg and VI should be greater than 14.5 MJ/kg (Ohm et al., 2015). The calculated value of CI and VI for DAN are 149.43 MJ/kg and 17.39 MJ/kg, respectively. This shows that DAN should not be used as an alternative fuel without prior treatment. After torrefaction, CI and VI for TAN252-60-5, are 21.93 and 13.44, respectively. Transportation and handling are noteworthy processes which involve during the conversion process of biomass. These processes are extremely influenced by flowing ability of biomass. The materials having angle of repose between 31-35^{o} have good flowing property and between 25-30^{o} have excellent flowing property, materials having HR between 1.19-1.25 have fair-flowing properties and between 1.12-1.18 have good flowing properties (Lumay et al., 2012), materials having CCI between 11-15, 16-20 and 21-25 have good, fair and passable flow behavior, respectively (Lumay et al., 2012; Szalay et al., 2015). The angle of repose for DAN and TAN252-60-5 are 38.39, and 35.75, respectively. HR and CCI are important parameters which depict flow behavior of material. The calculated value of HR for DAN and TAN252-60-5 are 1.29 and 1.21, respectively. CCI is a measure of bulk density, tapped density, moisture content, surface area and cohesiveness of biomass since it varies with all these parameters. CCI of DAN and TAN252-60-5 are 22.48 and 17.35, respectively. DAN torrefied at higher temperature has lesser tendency of agglomeration than the DAN, leading to better flow property. The flowing property of biomass can also be explained by cohesive forces (between the particles) and friction forces (between the wall and the particles) (Szalay et al., 2015). The cohesion coefficient of DAN and TAN252-60-5 are 0.40 and 0.35, respectively, which shows that after torrefaction cohesive force between the particle decreases, which favors the flowing behavior of TAN. This shows that fuel and flow properties of TAN moving toward the properties of coal, which makes it suitable as an alternative source of solid fuel or it, can be blend with coal.

5.3.6 BET surface area and density of raw and torrefied biomass

The surface area, pore diameter and pore volume of were obtained using the BET method. BET surface area, pore diameter and pore volume of TAN252-60-5 were found to be 0.9703 m^2/g, 13.69 nm and 0.0015 cm^3/g, respectively. Similar results were reported by Doddapaneni et al. (Doddapaneni et al., 2018) and Granados et al. (Granados et al., 2017). The variation of density of DAN and TAN252-60-5 are presented in Table 5.4. It was noticed that all three types of densities (bulk, tapped and particle) decreased as the temperature increased during torrefaction. The bulk, tapped and particle densities of DAN were 231.45, 300.71, and 1251 kg/m^3, respectively; and for TAN252-60-5, they were 193.48, 235.67, and 1156 kg/m^3, respectively. The release of volatile matter from DAN at higher temperature creates inside voids, which causes decrease in density along with increase in porosity of TAN. The TAN with increased surface area can be used as an adsorbent in many processes. Conag et al. (Conag et al., 2017) investigated the bulk and tapped density of switchgrass, sugarcane bagasse and sugarcane leaves. They found that bulk density of switchgrass varied from 50-264 kg/m^3 and bulk density of torrefied switchgrass varied from 68-325 kg/m^3 whereas bulk and tapped density of sugarcane bagasse varies from 46-87 kg/m^3 and 65-125 kg/m^3, respectively.

5.3.7 Thermogravimetric analysis

Figs. 5.4 (a) and (b) show the TGA and DTG analyses of DAN and TAN252-60-5. Each component of biomass (hemicellulose, cellulose and lignin) shows different thermal behavior; hence, they have different thermal degradation temperature. Hemicellulose and cellulose degraded at lower temperature between 200-350 ℃, while lignin decomposes at a wider temperature range between 280-600 ℃ (Ren et al., 2013a). Major mass loss in case of hemicellulose and cellulose occurs between 268 ℃ to 355 ℃ (Yang et al., 2007). Figs 5.4 (a) and (b) show that entire thermal degradation process can be divided into three zones viz. drying (1^{st} zone), devolatilization (2^{nd} zone) and char formation (3^{rd} zone). Drying zone corresponds to removal of moisture and light volatile matter whereas devolatilization zone corresponds to active pyrolysis of DAN or TAN. In char formation zone, disruption and demethylation of lignin leads to char formation (Collard & Blin, 2014). As a representative case, 20 % mass loss was observed for DAN at around 290 ℃; whereas, for TAN, it was observed at 353 ℃. This shift in decomposition temperature may be attributed to lower amount of hemicellulose present in TAN. The char yield in case of DAN is 21%, however in case of TAN252-60-5; char yield is 47%. This increase in char yield is also attributed to the decomposition of hemicellulose and limited decomposition of cellulose during torrefaction. The shoulder appeared in the DTG curve revealed decomposition of hemicellulose in case of DAN and generally, it was observed at around 300 ℃ (Müller-Hagedorn et al., 2003). In this study, similar shoulder can be seen in Fig. 5.4 (b) for DAN. In case of TAN252-60-5, shoulder disappeared, confirming that hemicellulose has already been degraded during torrefaction. Yang et al. (Yang et al., 2007) illustrated that peaks appeared in DTG curve with maximum weight loss, conforming the presence of cellulose in the biomass. The peaks in DTG curve for DAN and TAN can be seen at temperature around 360 ℃. Comparing DAN and TAN252-60-5, the intensity of peak in case of TAN252-60-5 is lower, confirming the degradation of cellulose in this range of temperature.

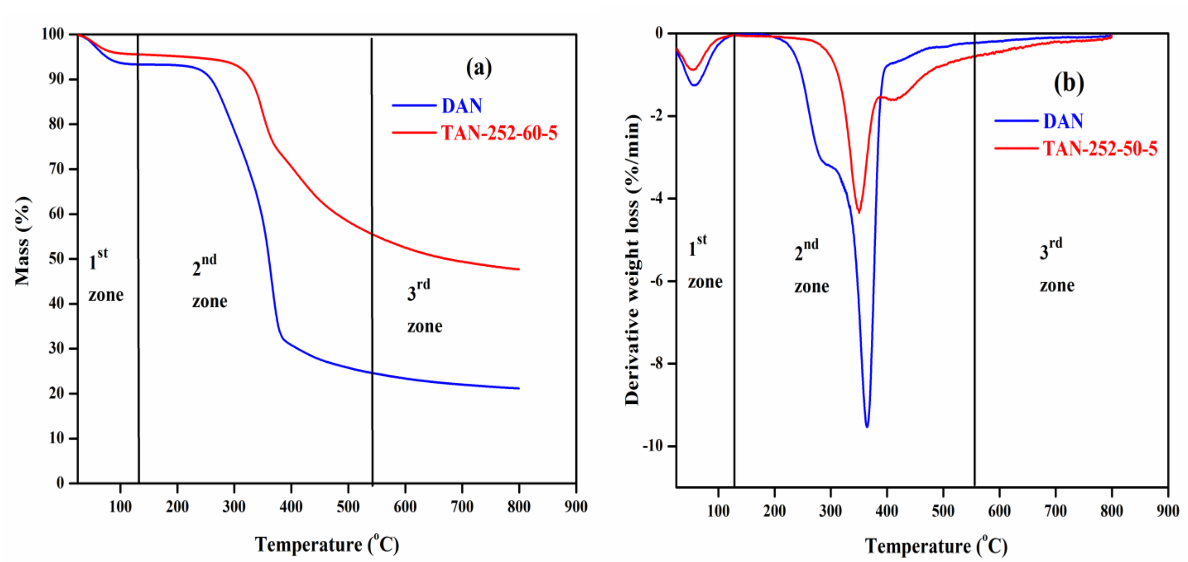

Figure 5.4 Thermogravimetric analyses of DAN and TAN252-60-5 (a) TGA (b) DTG

5.3.8 Fourier transform infrared spectroscopy (FTIR)

FTIR analysis was performed to observe the chemical changes in biomass due to torrefaction (Fig. 5.5). The structural and chemical changes in biomass are mainly due to decomposition of hemicellulose, which occurs mainly in the range of 200 ℃ to 300 ℃. In the wave number range from 4000 to 400 cm^{-1}, the functional groups of concern are O-H, C=O, C=C, C-H, and C-O-C. The characteristic peak between 3400-3100 cm^{-1} corresponds to stretching vibration of O-H bond (Gan et al., 2019) present mainly due to intra and intermolecular hydrogen bonding between alcoholic and phenolic groups present in cellulose and hemicellulose of biomass (Singh et al., 2019a). It can be observed that intensity of O-H bond in TAN250-60-5 has decreased due to torrefaction. Decrease in O-H bond intensity inferred disruption of hemicellulose during torrefaction. The decrease in intensity of peak between 2900-2750 cm^{-1} confirms the decrease of C-H bond stretching of aliphatic groups such as methyl and methelene compounds associated with alkanes and alkenes present in DAN (He et al., 2019). Decrease in intensity of peaks between 1750-1500 cm^{-1} may be attributed to deacetylation reaction, which causes decomposition of ester group present in hemicellulose (Carrasco & Roy, 1992). Between wave number of 600-700 cm^{-1}, intensity of peaks shows the presence of single and cyclic group of aromatic compound (Gomez-Serrano et al., 1996). Thus, as the process temperature increases, the intensity of peaks decreases for TAN252-60-5 in comparison to DAN, conforming structural change of chemical compounds present in DAN like water molecules, carboxyl groups, esters, aldehydes, ketones, acids and aromatic compounds.

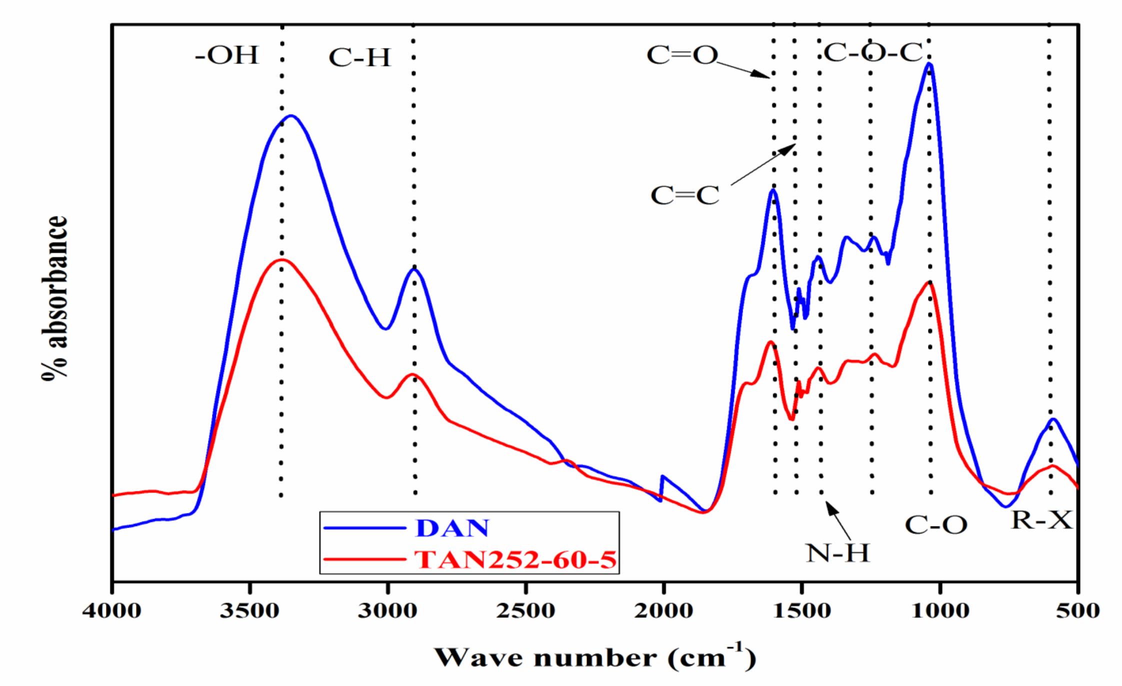

Figure 5.5 FTIR spectra of DAN and TAN252-60-5

5.3.9 Scanning electron microscope (SEM) and energy dispersive X-ray (EDX) analysis

To understand the influence of torrefaction on morphology of biomass, the scanning electron microscope images of DAN and TAN252-60-5 with 5000 magnification are presented in Fig. 5.6. The impact of thermal pretreatment could be seen in Fig. 5.6 (c). Generally, hemicelluloses are branched polysaccharides which contain strong bulky and branched tissues of xylem (Ibrahim et al., 2013). Branched structure on the surface of the DAN elucidates the presence of hemicellulose (Fig. 5.6 (a)). However, in case of TAN, these branched structures started disappearing, suggesting degradation of hemicellulose during torrefaction. The presence of pores is clearly visible for TAN252-60-5. The generation of pores in case of TAN252-60-5 is attributed to lower particle density than

DAN, which may decrease the grinding energy requirement for size reduction of DAN and increase in surface area. These are in agreement with the results reported by Ibrahim et al. (Ibrahim et al., 2013), Bach et al. (Bach & Skreiberg, 2016). Energy dispersive X-ray analysis is used to detect chemical elements present in the sample and to approximate their relative abundance. The EDX images of DAN and TAN252-60-5 are shown in Figs. 5.6 (b) and (d). It can be observed that in case of TAN252-60-5, some useful elements like Nitrogen (N), Calcium (Ca), Magnesium (Mg) and Potassium (K) appear with higher peak intensity along with Carbon (C) and Oxygen (O) than DAN indicating densification due to torrefaction. Oxygen gets reduced due to removal of –OH bonds, which is also supported by the FTIR analysis (Fig. 5.5). The increase in carbon content is also supported by enhanced fixed carbon content due to torrefaction, as presented in Table 5.4.

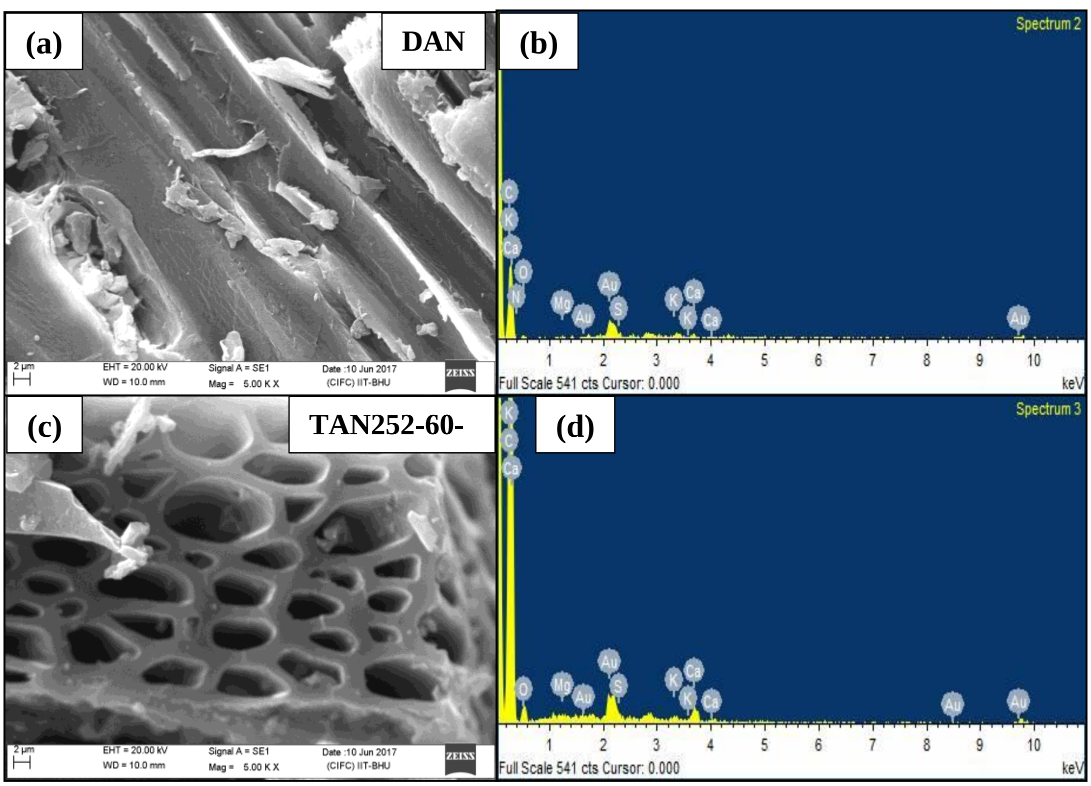

Figure 5.6 SEM and EDX images: (a) and (b) for DAN, (c) and (d) for TAN252-60-5

5.3.10 X-Ray diffraction (XRD) analysis

The major components of biomass are hemicellulose, cellulose and lignin. Among these, hemicellulose and lignin are amorphous in nature and cellulose is crystalline (Zheng et al., 2015). To investigate the effect of torrefaction on crystalline nature of DAN and TAN252-60-5, XRD analysis was performed and crystallinity index (CrI), FWHM of (002) peak and crystal size (L_{002}) were also calculated. The results are shown in Fig. 5.7 and Table 5.5. At 2θ = 22°, the strongest peak with highest intensity originated from 002 crystalline plane. It was observed that relative peak intensity of TAN252-60-5 is lower than the DAN. This shows that crystallinity of biomass decreased after torrefaction. Also, CrI of DAN and TAN252-60-5 was found to be 44.97 and 40.29 %, respectively, which confirm the decrease in crystallinity. The decrease in crystallinity might be due to disruption of intermolecular hydrogen bonding (Wannapeera & Worasuwannarak, 2015) and degradation of cellulose during torrefaction. FWHM of (002) peak increases in case of TAN252-60-5 with respect to DAN. The crystal size decreases in case of TAN252-60-5. Thus the crystal size of biomass decreases upon torrefaction. Similar results were obtained many researchers. Zheng et al. (Zheng et al., 2015) investigated the effect of torrefaction on crystalline behavior of corncob. They found that, at mild torrefaction, CrI of torrefied corncob increased, while at severe torrefaction CrI decreased due to degradation of crystalline cellulose of corncob. Similar results were also obtained by Wen et al. (Wen et al., 2014) during torrefaction of Bamboo.

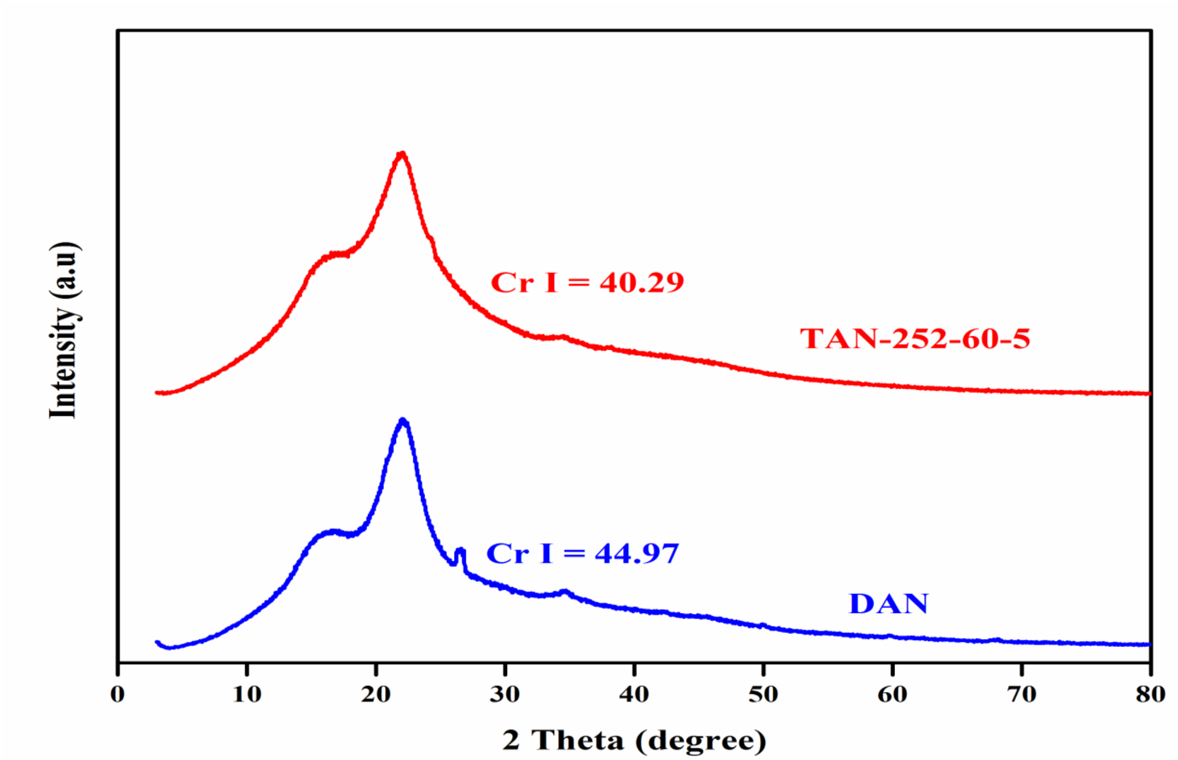

Figure 5.7 XRD spectra of DAN and TAN252-60-5

Table 5.5 Crystalline parameters of DAN and TAN252-60-5

Sample	CrI (%)	2θ (degree)		β^a(degree)	L_{002} (nm)
		I_{002}	I_{am}		
DAN	44.97	21.8	14.9	9.7	0.87
TAN252-60-5	40.29	21.7	14.5	11.5	0.73

[a] Full width at half maximum (FWHM) of (002) peak

5.3.11 Moisture absorption

Fig. 5.8 shows the percentage of moisture absorbed by DAN and TAN252-60-5. DAN and TAN252-60-5 absorbed 8.15 and 4.51 % moisture, respectively from open environment (average relative humidity of 60% ±3) when kept for one day. After 5 days, percentage of moisture absorbed by DAN, and TAN252-60-5 are 34.44, and 7.12%, respectively. The water absorption capacity of biomass is associated with the amount of hemicellulose present in biomass. Hemicellulose contains many hydroxyl group (-OH) which compel biomass to be polar and form hydrogen bonds with water molecules easily. Due to torrefaction, hydroxyl bonds (-OH) in biomass are dissociated and became unsaturated having non-polar characteristics, which diminishes the attraction of biomass to form hydrogen bonds with water molecules (Bach & Skreiberg, 2016). TAN252-60-5 may also absorb less moisture due to deposition of tar, condensing on the surface (Ohm et al., 2015). Tar deposition prevents the capillary rise of water molecules due to blockage of pores inside TAN252-60-5. The torrefaction makes biomass hydrophobic so that it engrosses lesser moistness and offers more stability to biomass when kept in open environment. This suggests that TAN obtained at higher temperature can be stored like coal in open environment, which significantly reduces transport, storage and handling cost of biomass.

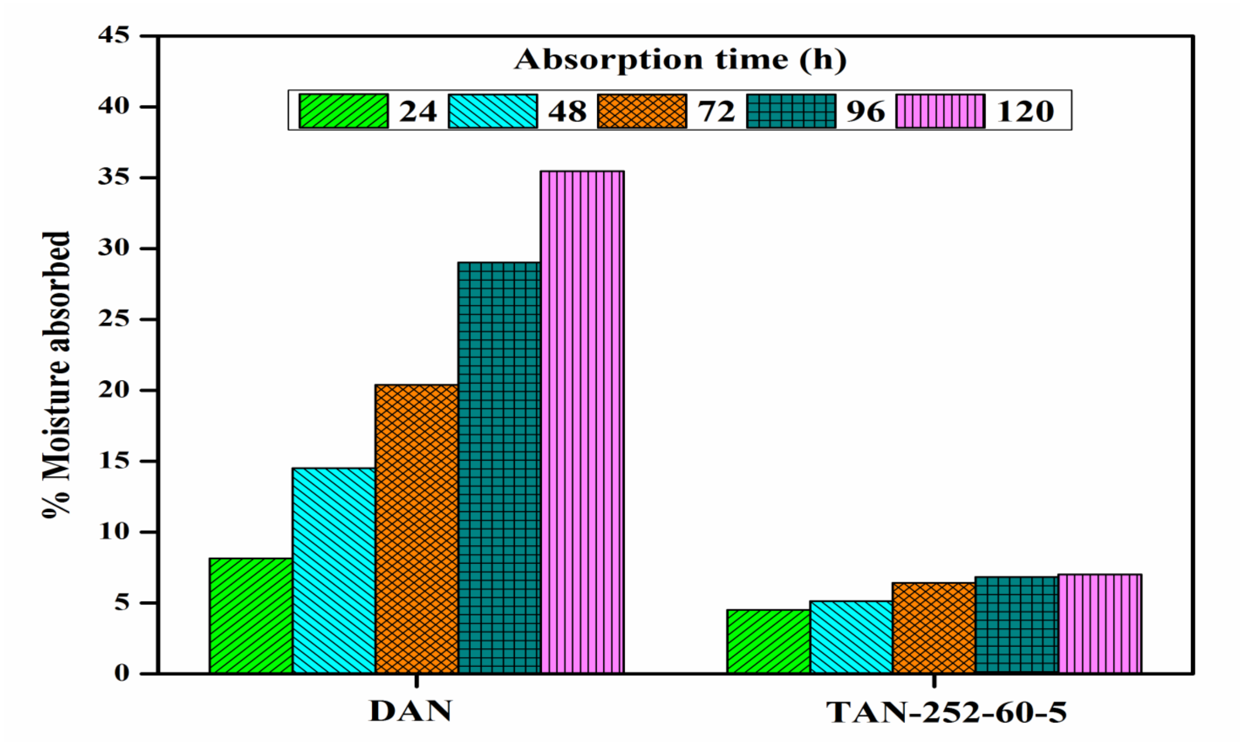

Figure 5.8 Moisture absorption characteristics of DAN and TAN252-60-5.

5.4 Conclusions

The torrefaction of *Acacia nilotica* was carried out in a laboratory scale fixed-bed reactor. The process parameters like temperature, retention time and heating rate were optimized for HHV and EY. A different set of parameters were obtained in case of optimum HHV and EY of TAN individually. The optimum value of temperature, retention time and heating rate to obtain maximum value of HHV and EY combined, were 252 ℃, 60 min, and 5 ℃/min, respectively. It was noted that the effect of temperature on torrefaction was significant, while effect of retention time and heating rate were minimal. Besides, the physical and chemical properties of DAN improved due to torrefaction. For example, MC, H/C ratio and O/C ratio decreased by 73.23, 52.94 and 46.22 %, respectively; whereas FC content and HHV increased by 75.54 and 18.62 %, respectively. FR increased by 87.39 %; whereas, CI and VI decreased by 83.32 and 22.71 %, respectively. Flow properties such as angle of repose, HR, CCI and cohesion coefficient (C) decreased by 8.04, 6.20, 22.48, and 12.5 %, respectively. Bulk, tapped and particle densities of TAN252-60-5 were decreased by 16.4, 21.62 and 7.59 %, respectively. Moisture sorption test confirmed that TAN252-60-5 absorbed 27.32 % less moisture than DAN when kept in open environment at comparable relative humidity. TGA study suggests that onset of devolatilization shifted to higher temperature in case of TAN and char yield increased during pyrolysis of TAN. Torrefaction has greatly enhanced surface defects and reduced crystallinity of biomass as revealed by SEM-EDX and XRD analysis individually. Overall, it may be concluded that optimization of torrefaction process favors two aspects; first, it may reduce the operational cost during the scaling of process at industrial level. Secondly, TAN has much improved properties than DAN, which can increase the process efficiency during its utilization in pyrolysis, gasification and co-pyrolysis with coal in thermal power plants.